† Electronic Supplementary Information (ESI)

Large-scale synthesis of bismuth hollow nanospheres for highly efficient Cr(VI) removal

Fan Qin,[a] Guangfang Li,[a] Hao Xiao,[a] Zhong Lu,[a] Hongzhe Sun,[b] and Rong Chen*[a]

[a] *Key Laboratory for Green Chemical Process of Ministry of Education and School of Chemical Engineering and Pharmacy, Wuhan Institute of Technology, Xiongchu street, Wuhan, PR China*

[b] *Department of Chemistry, The University of Hong Kong, Pokfulam Road, Hong Kong SAR, PR China.*

* Corresponding author. Tel.: (+86)13659815698; fax: (+86)2787195671.

E-mail address: rchenhku@hotmail.com (Prof. R. Chen)

Experimental section

Materials: Bismuth nitrate pentahydrate ($Bi(NO_3)_3 \cdot 5H_2O$) was purchased from Aladdin, ethylene glycol (EG) and nitric acid (HNO_3) were obtained from Sinopharm Chemical Reagent Co. (China). Poly(vinylpyrrolidone) (PVP, M_w=10,000) was purchased from Sigma-Aldrich Inc. Potassium bichromate ($K_2Cr_2O_7$) was purchased from Aladdin. All the reagents were analytical grade and used directly without further purification.

Synthesis of bismuth hollow nanospheres: In a typical experimental procedure, $Bi(NO_3)_3 \cdot 5H_2O$ (0.182 g, 0.375 mmol) was dissolved in HNO_3 solution (5 mL, 1 M), then PVP (0.15 g, 0.015 mmol) and EG (25 mL) were added into this solution. Then the mixture was transferred into a stainless steel autoclave with Teflon liner. The autoclave was sealed and maintained at 150 °C for 12 h. The obtained products were centrifuged and washed with deionized water and finally dried in a desiccator for a few days for further characterizations. Other samples were also prepared under different reaction conditions (Table S1).

Table S1 Experimental condition for the synthesis of bismuth nanostructures.

Sample	The amount of PVP (g)	solvent
S1	0.15	EG
S2	0	EG
S3	0.3	EG
S4	0.45	EG
S5	0.15	H_2O

Characterization: The obtained products were characterized by X-ray diffraction (XRD, Bruker D8 advance), scanning electron microscope (SEM, Hitachi S4800), transmission electron microscope (TEM, Philips Tecnai G2 20) with an accelerating voltage of 200 kV and BET analysis (Micromeritics ASAP 2020).

Cr(VI) removal experiments: Solutions containing different concentrations of Cr(VI) was prepared using $K_2Cr_2O_7$ as the Cr(VI) source. In a typical adsorption procedure, 0.02 g of as-prepared Bi samples was added to 20 mL of the above solution under stirring. At each given time interval, the suspension was sampled (2 mL) and centrifuged to remove the Bi powders. The concentration of Cr(VI) during the adsorption was measured with a Shimadzu UV2800 spectrophotometer. All of the measurements were carried out at room temperature.

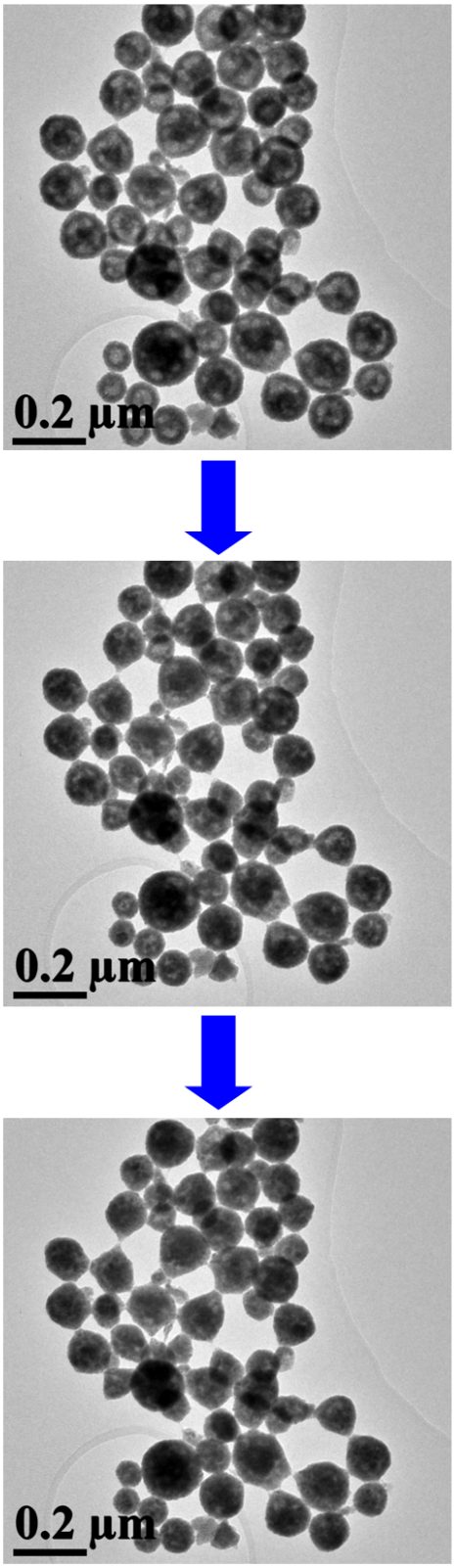

Fig. S1 The morphology evolution of Bi nanospheres with the increasing of electron beam irradiation time.

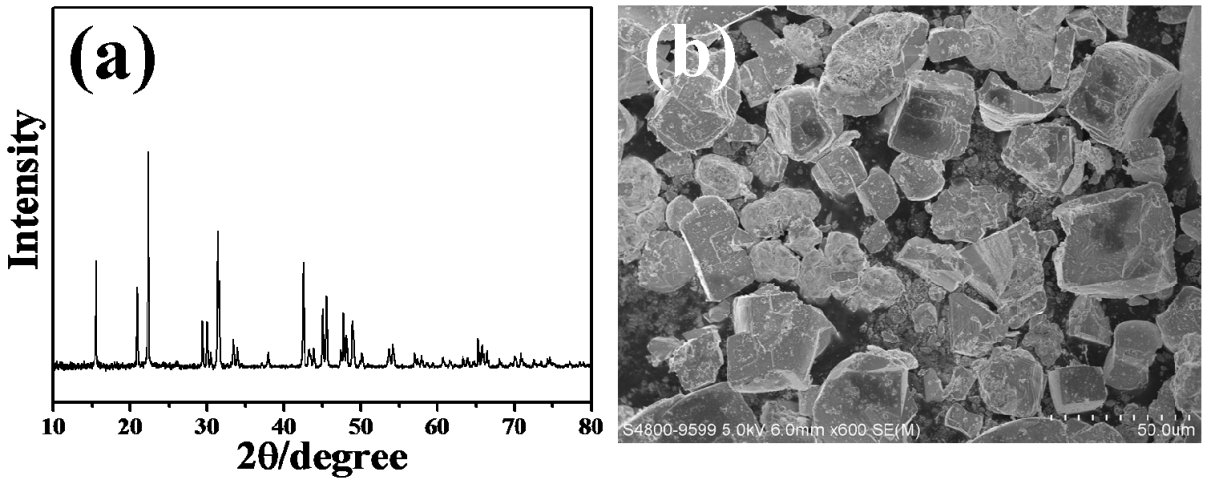

Fig. S2 (a) The XRD pattern (b) and SEM image of the sample obtained in deionized water (**S5**).

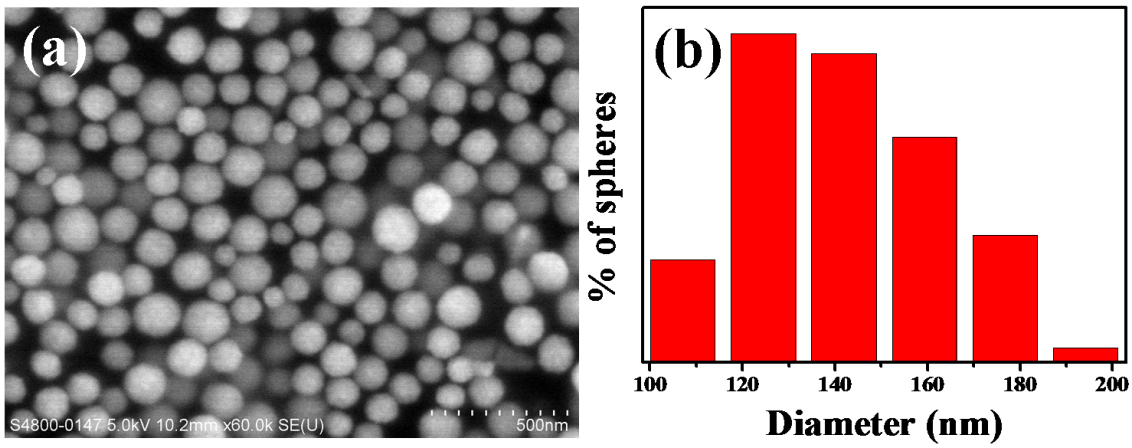

Fig. S3 (a) SEM image and (b) the histogram of size distribution of sample S4.

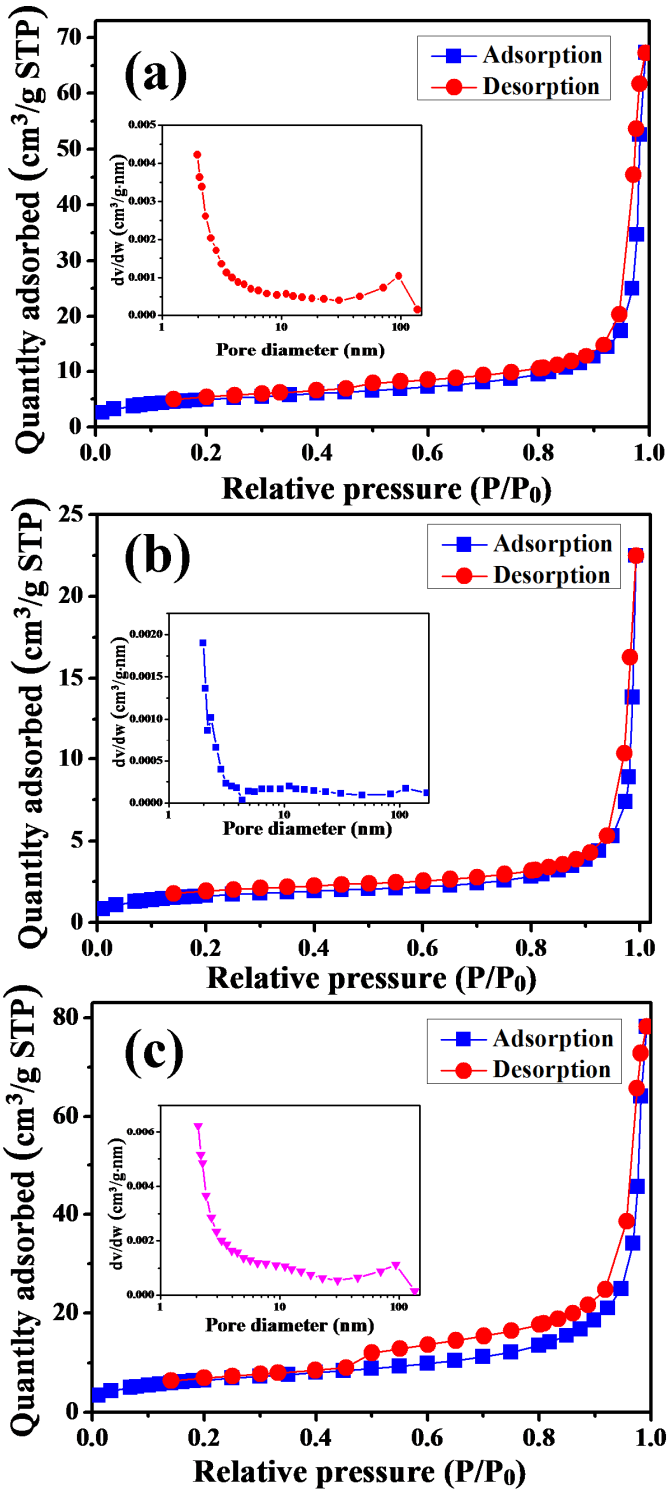

Fig. S4 Nitrogen adsorption and desorption isotherms and corresponding pore-size distribution curves (insets of Fig. S5a-S5c) of the Bi samples (a) **S1**, (b) **S2**, (C) **S3**, respectively.

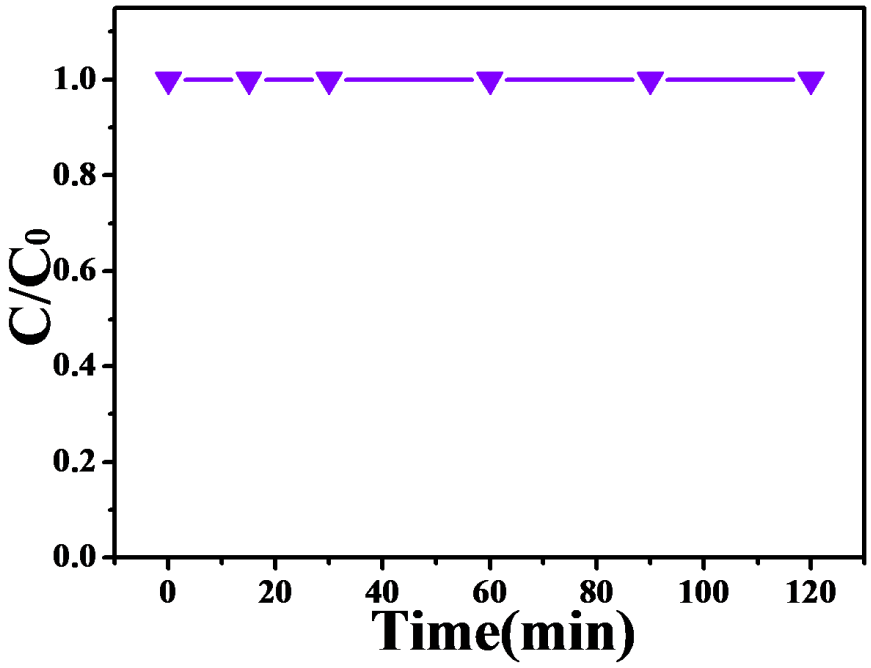

Fig. S5 Absorption rate of Cr(VI) solution (initial concentration of 30 mg/L) in the presence of commercial Bi sample.

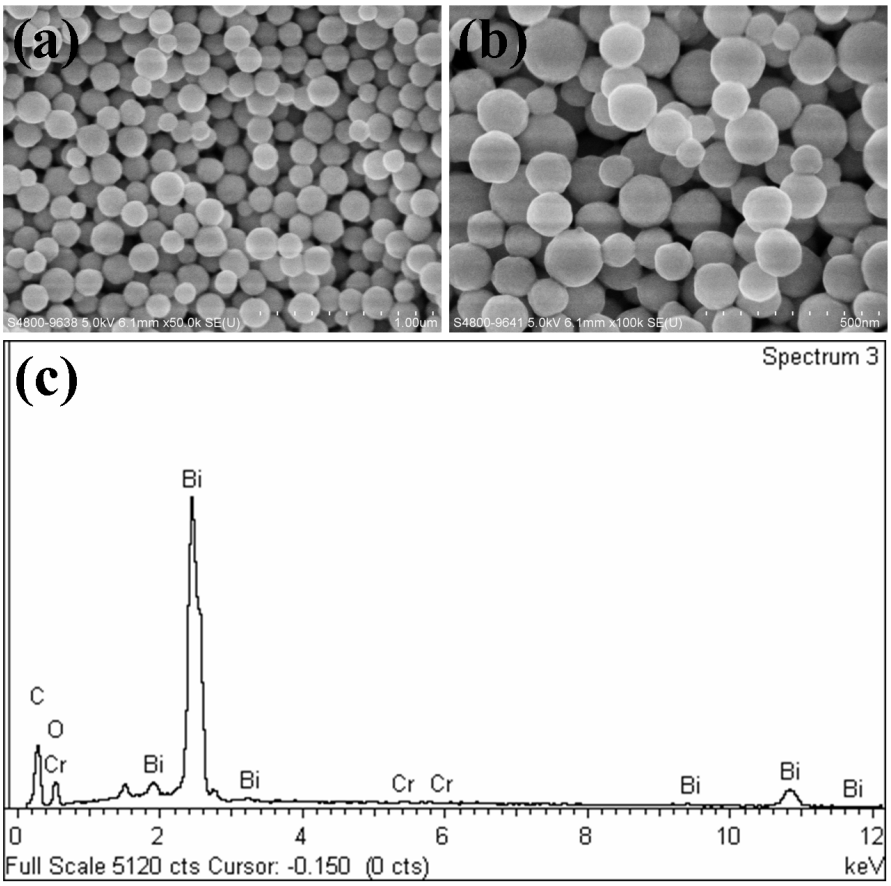

Fig. S6 (a, b) The SEM images and (c) EDX of the sample S1 collected after adsorption Cr(VI).

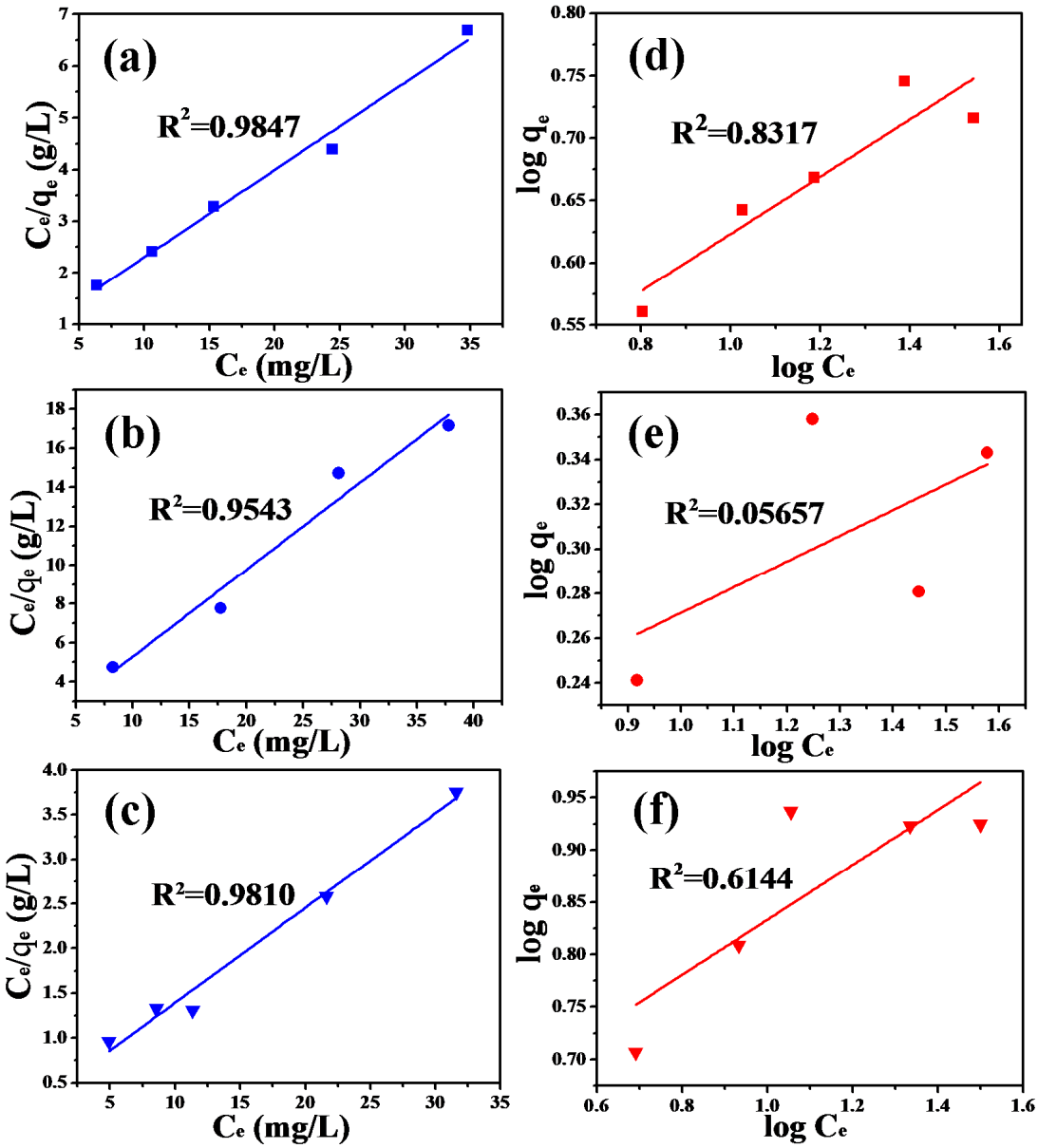

Fig. S7 Cr(VI) adsorption models of Bi nanospheres: Langmuir isotherm plots of sample (a) **S1**, (b) **S2**, (c) **S3**, respectively; Freundlich isotherm plots of sample (d) **S1**, (e) **S2**, (f) **S3**, respectively.

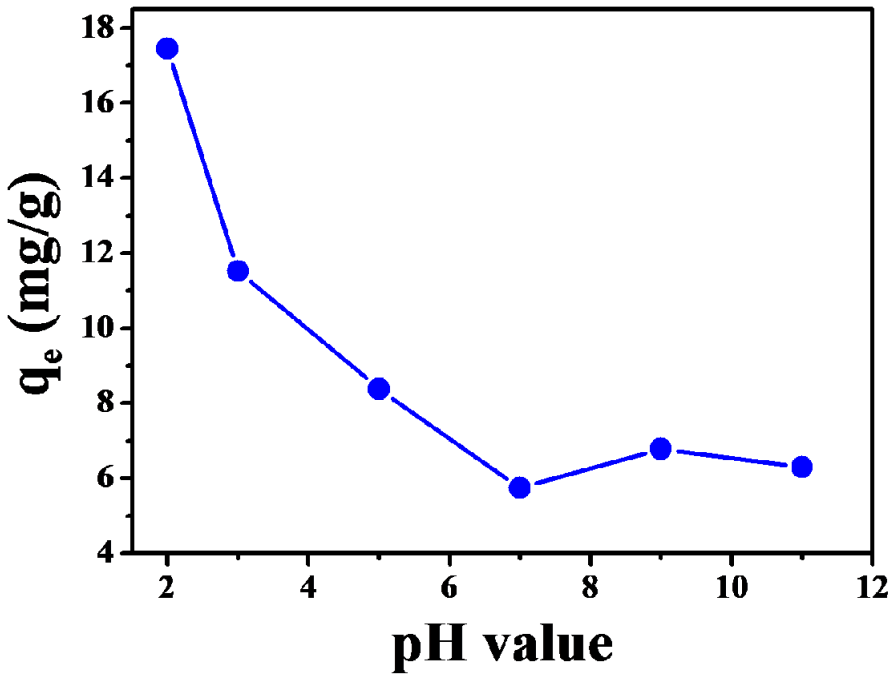

Fig. S8 Effect of pH value of initial solution of Cr(VI) (initial concentration of 30 mg/L) on removal capacity of Bi sample (**S3**).

Table S2 Estimated dimensionless separation factor (R_L) of the Bi nanospheres.

Sample	$R_L=1/(1+bC_0)$			
	C_0 =10 mg/L	C_0 =20 mg/L	C_0 =30 mg/L	C_0 =40 mg/L
S1	0.267	0154	0.108	0.083
S2	0.154	0.083	0.057	0.043
S3	0.238	0.135	0.094	0.072